ISSN: 1304-7981 Number: **12**, Year: **2016**, Pages: **159-169** **http://jnrs.gop.edu.tr**

Gaziosmanpasa University
Graduate School of Natural and Applied Sciences
Journal of New Results in Science

Received: 15.05.2016
Accepted: 30.09.2016

Invited Editor: Mahmut Hekim
Area Editor: Zafer Dogan

The Performance Analysis of an Air Gapped Transformer Used in Wireless Charging System for Shuttle Robot

Ahmet Fenercioğlu[a,1] (ahmet.fenercioglu@gop.edu.tr)
Elif Özkan[b], (eingenc@diren.com)
Salih Can Demiryürek[b] (sdemiryurek@diren.com)

[a]Gaziosmanpasa University, Department of Mechatronics Engineering 60150 Tokat, Turkey
[b]Dimak Diren Makine Ar-Ge Ltd. Şti., Tokat Technology Development Zone, 60250 Tokat

Abstract - This study included performance analysis studies of an EE core structured and air gapped transformer which is operated under the network frequency for wireless charging battery of shuttle robots during duty. Proposed design is modeled analytically and design is verified by 2 dimensional finite element analysis (FEA) and experiments. In this stage no loaded, full loaded, and short circuit analysis of model are simulated and performance is determined according to air gap distance. Primary and secondary currents, voltages, power factor, efficiency, active power, regulation and short-circuit ratios are examined by analysis and experiments. In FEA solutions, input power is 588,28 W, output power is 387,89 W, power factor is 0.31, regulation is 30,88 %, short-circuit ratio is 70,78 % for 3 mm air gap distance. The air-gapped transformer was used in wireless charge station (WCS) and tested. About 63 V voltage and 4.24 A current are applied to Pb-Ac battery group by WCS. 200Wh energy is transferred wirelessly along 45 minutes.

Keywords –
air gapped transformer, wireless transformer, transformer experiments, wireless charge, E core

1. Introduction

Cartesian robot commonly used in robotic storage systems. This robot makes to transfer the pallets in 3 axes for loading and unloading the storage cells. This robot system consist one aisle robot that carry the storage aisle in two axes and pallet robot that is as a separate platform to transfer the pallets aisle robot and storage cells. Pallet robot is working with battery. To make continuous duty of this robot, meantime it is waiting on the aisle robot; it is intended to be charged wirelessly. The aisle robot and pallet robot pictures are shown in Figure 1.

[1]**Corresponding author**

Journal of New Results in Science 12(2016) 159-169

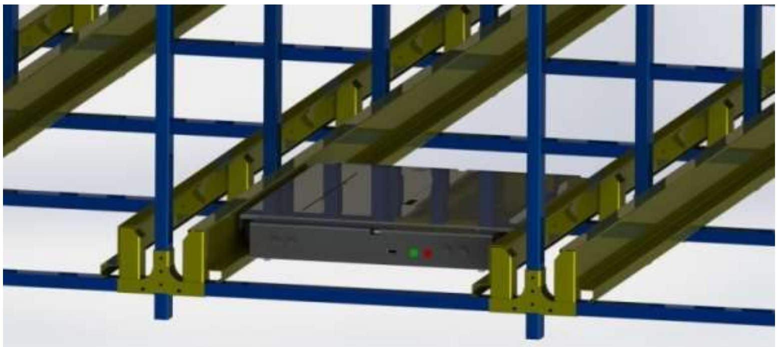

Figure 1. Shuttle robot

In wireless charging systems, transfer power from a greater distance use of high frequency system is common. In the literature, it is prescribed specifically mentioned system of electric vehicle batteries can be charged during parking.

Takanashi and friends [1] performed power transfer for the electric vehicle, to make a 20 cm air gap for the 3 kW transformer with high frequency in study. In this study using H shaped core and a separate primary capacitor, to provide a yield of %90 power transfer [1].

Li and friends [2] in the review of the literature, they stated, at the high frequency %90 and higher yield kW level of power can be transferred wirelessly to the electric vehicle successfully. With their works, highly efficient energy transfer of the wireless charging station (WCS) which will encourage researchers in this area [2].

Bloom and friends [3] in their study they examined design process of wireless a productive level 2 battery charging systems. They designed a new AC-DC rectifier, a boosting converter permanently modified regulation and hysteresis controller. They obtained %80 efficiency of the WCS system under full load from 15-25cm distance [3].

This study is envisaged for use EE core structure and air gapped transformer at the WCS. A transformer is designed to transfer power at the main frequency due to the close air gap distance wireless power to be transferred. In the system, primer side is on the aisle robot, secondary side is on the shuttle robot was located. When shuttle robot is getting on the aisle robot, as soon as secondary and primary core mutual positioning charging will start. At the time they separate, charging system will switch to standby mode. The system layout is shown in Figure 2.

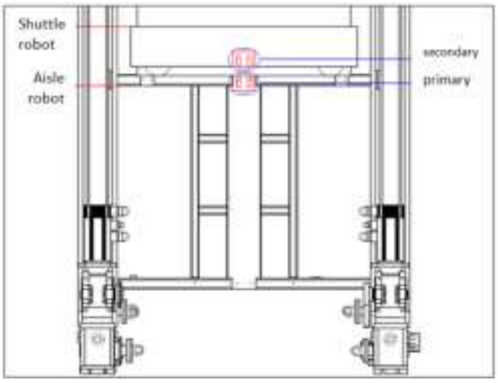

Figure 2. System layout

2. Material and Method

Power transfer system envisaged for the WCS is EE core structure and air gapped transformer. System operation is based on Faraday's principle of the transformer. Induced electromotive force (emf) in the secondary according to Faraday's law of value is given in Eq.1.

$$E = 4.44 \times \phi \times F \times N \tag{1}$$

ϕ is magnetic flux in the air gap (Wb), F is frequency (Hz) and N is number of secondary winding turns. Frequency is increased to transfer power from the large air gap. But a transformer is used which runs at 50 Hz network frequency because in the robot charging application a maximum of 5mm air gap is enough, cost reduction and negative impact of electrical noise at high frequency. The transformer and 3D model of the system is given in Figure-3.

a) b)

Figure 3.a) 3D design model b) transformer cores and windings

Reluctance is affected so much due to wide gap at the magnetic equivalent circuit. Therefore, reluctance of core is not taken into consideration. Magneto motive force (mmf) the primary and secondary windings are provided, respectively F_1 and F_2.The reluctances of the air gap are R_{g1}, R_{g2}andR_{g3}. Magnetic circuit and EE cores are shown in Figure 4.

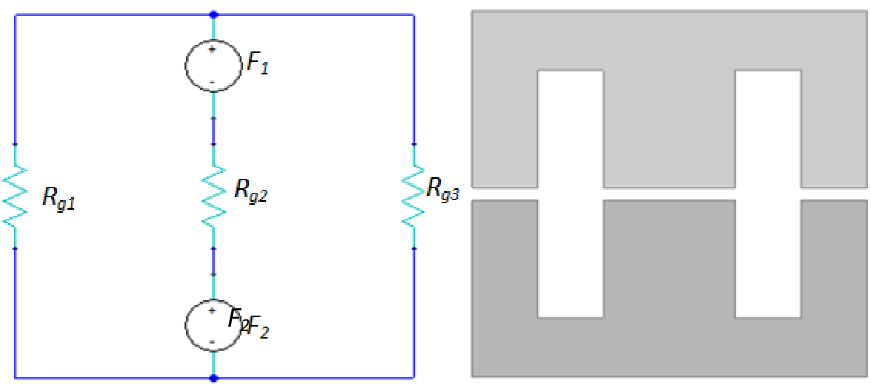

a) b)

Figure 4. a) Magnetic equivalent circuit b) EE core

According to equivalent circuit and geometric dimensions of core; l_g air gap distance (m), A_g flux path section (m²) as were obtained. Cross section of flux path in the air was 10% higher than the core section due to the fringing influence. Magnetic permeability of the gap is $\mu_0 =$

Journal of New Results in Science 12(2016) 159-169

$4\pi 10^{-7}$ H/m. Reluctance of the air gap is calculated with Eq. 2 and total reluctance is calculated with Eq. 3.

$$R_{g_1} = \frac{l_{g1}}{\mu_0 \times A_{g1} \times 1.1} \tag{2}$$

$$\sum R_g = \frac{R_{g_1} \times R_{g_2}}{R_{g_1} + R_{g_2}} + R_{g_3} \tag{3}$$

Magnetic flux is obtained from Eq. 4. When the air gap is increasing reluctance grow. This situation reduce the magnetic flux and hence the reduction in secondary emf seen as Eq. 1 and Eq. 4.

$$\emptyset = \frac{F_1 + F_2}{\sum R_g} \tag{4}$$

T equivalent circuit of the transformer is shown in Figure5.

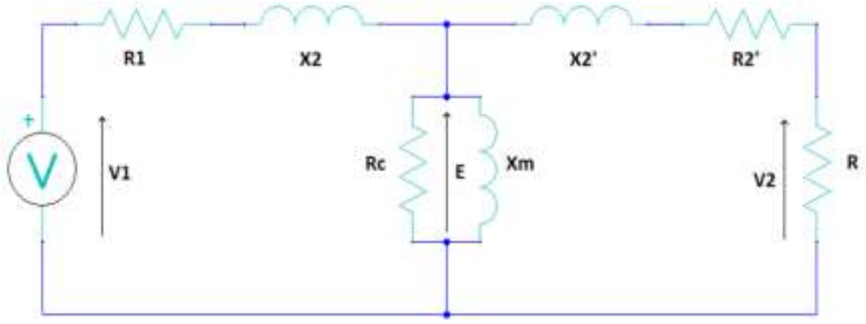

Figure 5. Electrical T equivalent circuit of transformer

Located equivalent circuit parameters are respectively, R_1 primary resistance (ohm), X_1 primary leakage reactance (ohm), R_2' reduced secondary resistance (ohm), X_2' reduced secondary leakage reactance (ohm), R_c core resistance (ohm), X_m magnetizing reactance (ohm), V_1 primary voltage (volt), V_2 secondary voltage (volt).

To determine proposed the system performance, simulations are made by no-load, full load and short circuit tests work. Distance of the air gap was measured the effect of regulation of no-load operation, terminal voltage in loaded operation, effects on primary and secondary current and in the short-circuit test the effects of the relative short circuit voltage.

Primary voltage is set until secondary current transfer at full load, secondary terminals shorted by at short circuit test. Relative short circuit voltage was measured, this current measured primary voltage and the rate of nominal input voltage of short circuit voltage (V_k) is calculated according to Eq. 5.

$$\%U_k = \frac{U_k}{U_1} \times 100 \tag{5}$$

In the no-load work test, load has been removed in the secondary terminals and voltage measured by the air gap changes. The % regulations were found terminal voltage of the full load (V_2) and no-load (V_0) according to Eq. 6.

$$\%R_g = \frac{V_0 - V_2}{V_2} \times 100 \quad (6)$$

The performance of the system is determined the secondary which is calculated wirelessly transmitted active power, power factor and efficiency values at the full load test run. All data were obtained by the finite element method (FEM) to determine the performance of the system.

WCS system consists of air gapped transformer, controlled AC/DC rectifier, controller and battery group. Block diagram of WCS is shown in Figure 6.

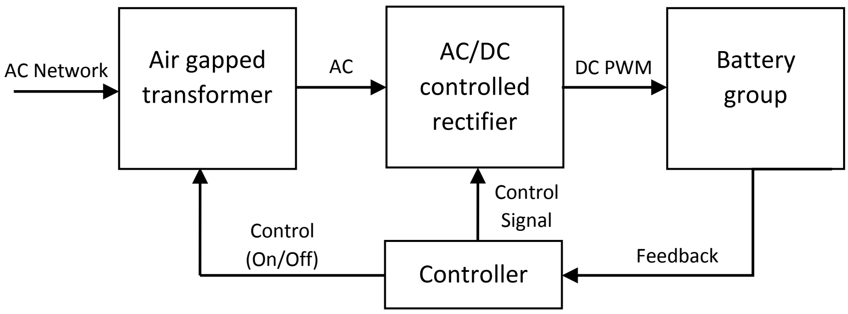

Figure 6. Block diagram of WCS

AC network (220 V, 50 Hz) is applied to primary winding of air gapped transformer. 60 - 110V AC voltage is taken from secondary winding according to air gap distance (0-5 mm) terminals and applied to AC/DC controlled rectifier. Rectifier switching signals and primer On/Off control signals are provided by controller accordance with battery voltage and winding temperature. Air gapped transformer's experiments were made with air gap distance change for no load and full load operations. The WCS experimental setup is shown in Fig.7.

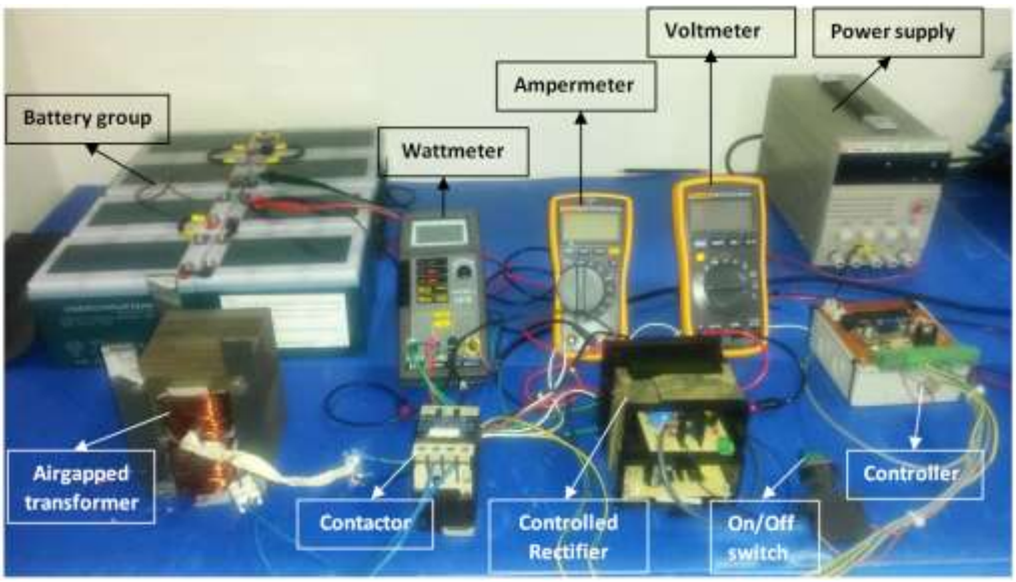

Figure 7. WCS experimental setup

3. Results and Discussion

Standard transformer tests were done with FEA and measurements in order to determine the performance of the WSC. In all analyses and experiments solutions were performed air gap varying between 0-5 mm each 1mm.

3.1. Full Load Analysis

10 ohm fixed ohmic load is connected to the secondary in full load test of WCS. Current, voltage, efficiency, $\cos\phi$ and flux linkage has been investigated performing the FEM analyses according to the varying the air gap. The rms values of the primary and secondary current are graphically presented in Figure 8 according to the air gap. As a result of increasing the air gap reluctance value decreases and the inductance value increases. This situation is reflected in the Eq.7.

$$L=N^2/R \tag{7}$$

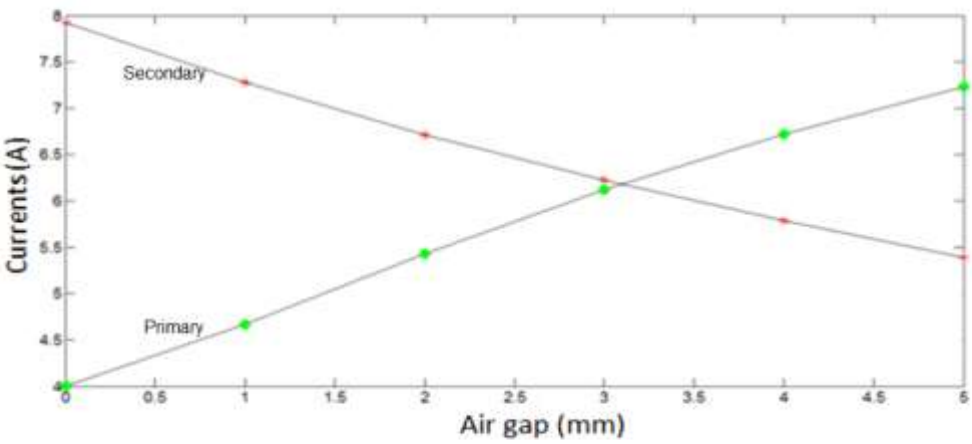

Figure 8.Current versus air gap distance

Primary current by increasing the air gap is increased due to the magnetizing current and secondary current is reduced. The impact on flux linkage of varying air gap is given in Fig.9.

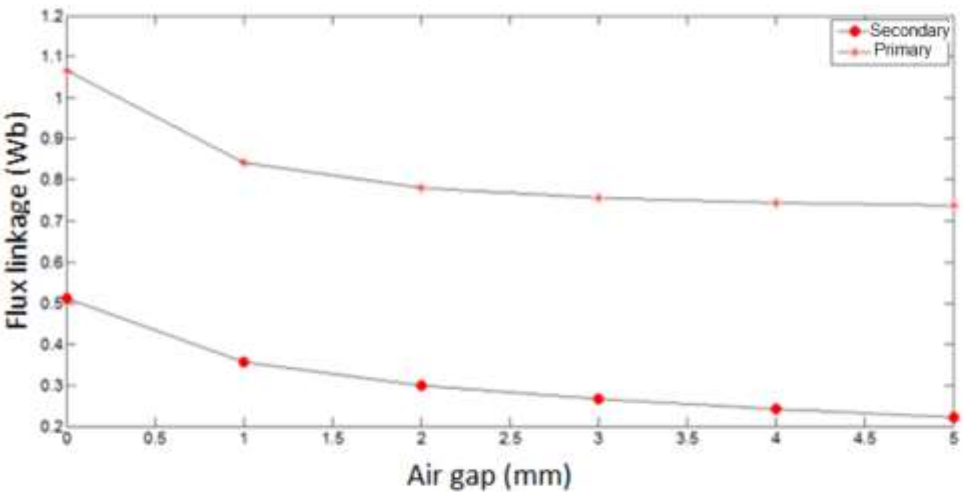

Figure9. Flux linkage versus air gap distance

In this case; inductive current is increased. At the same time increasing the magnetizing current reduces the power factor. Figure 10 is seen in the *cosφ* decrease because of increasing reluctance value with the air gap.

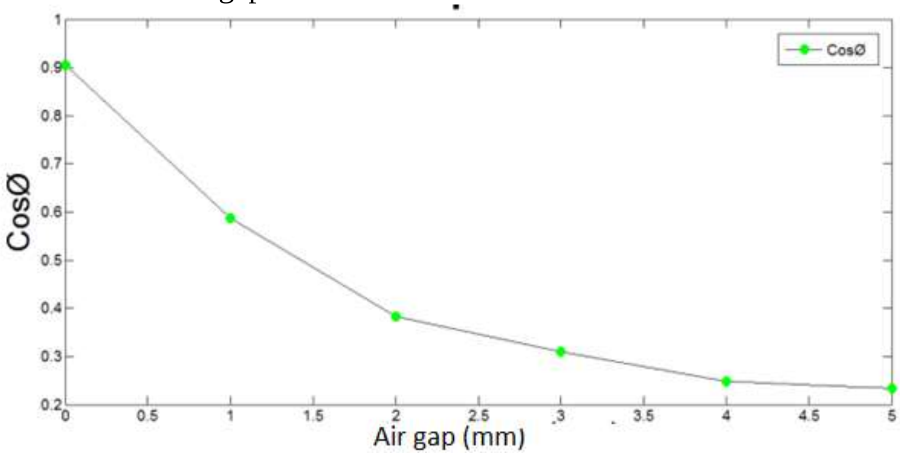

Figure 10. Power factor (Cosφ) versus airgap distance

The increased air gap reduces voltage which drops on the secondary side. It is shown in Fig. 11.

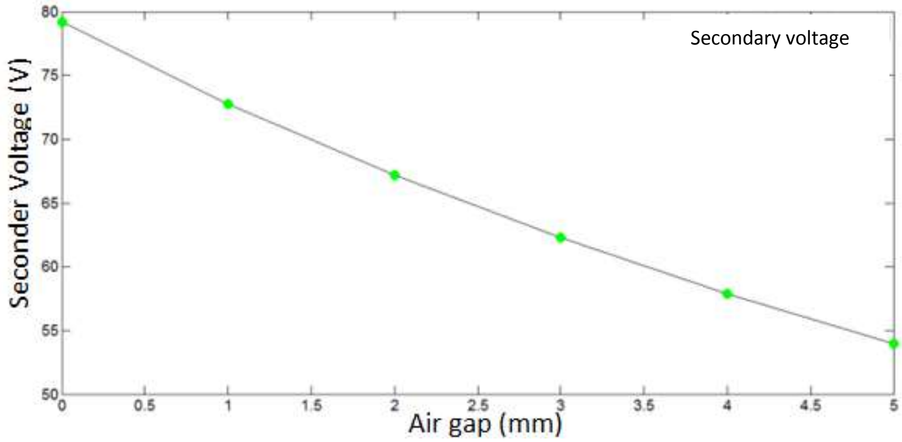

Figure 11.Secondary voltage (V_2) versus airgap distance

Efficiency decrease as shown in Figure 12 active power reduced taken from output due to lower cos*φ*.

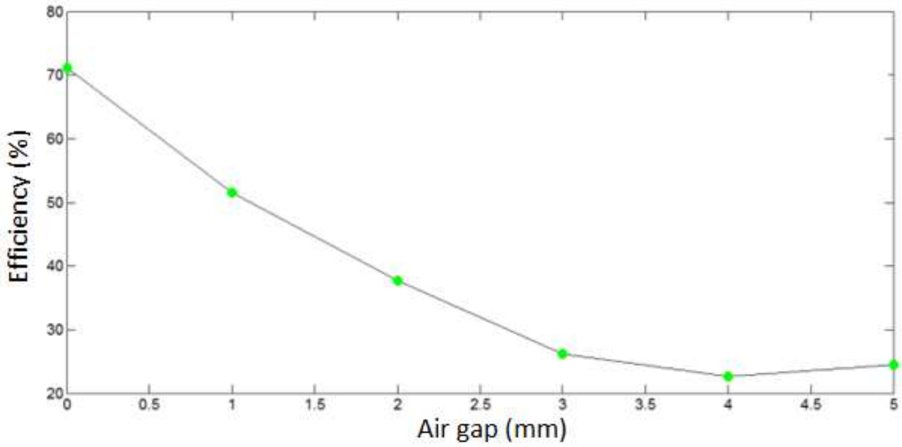

Figure 12. Efficiency versus airgap distance

3.2. Short Circuit and No-load Analysis

Current, voltage, power and cos*φ* values are presented each air gap distance of made short circuit and no-load analysis results are given in Table 1. Voltages and currents results are shown in Figures 13-15 for short circuits, no-load and full load operations

Table 1. Short circuit and no-load analysis results

	Short circuit				No load			
l_g (mm)	V1 (V)	I2 (A)	P_k (W)	cosφ	V2 (V)	I_1 (A)	P_o (W)	cosφ
0	92,02	7,9	187.41	0.509	105,82	0,65	115.83	0.81
1	99,09	7,9	160,29	0.368	98,97	2,54	328	0.587
2	109,71	7,9	183,08	0,338	90,44	3,94	390	0.45
3	116,79	7,9	200,54	0,323	81,51	4,93	399	0.368
4	125,29	7,9	225,95	0,314	76,75	5,86	417	0.324
5	134,48	7,9	258,59	0,309	71,05	6,55	446	0.31

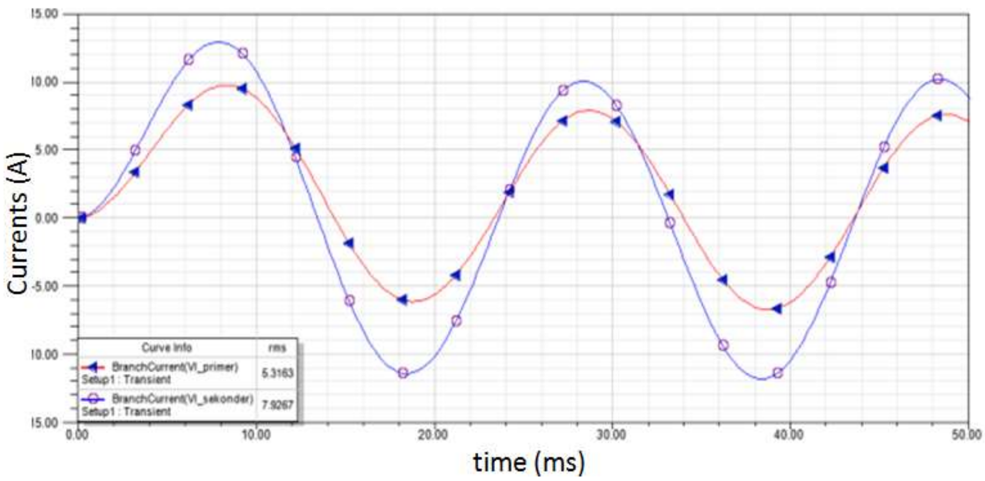

Figure 13. Voltage, current curves in short circuit

Journal of New Results in Science 12(2016) 159-169

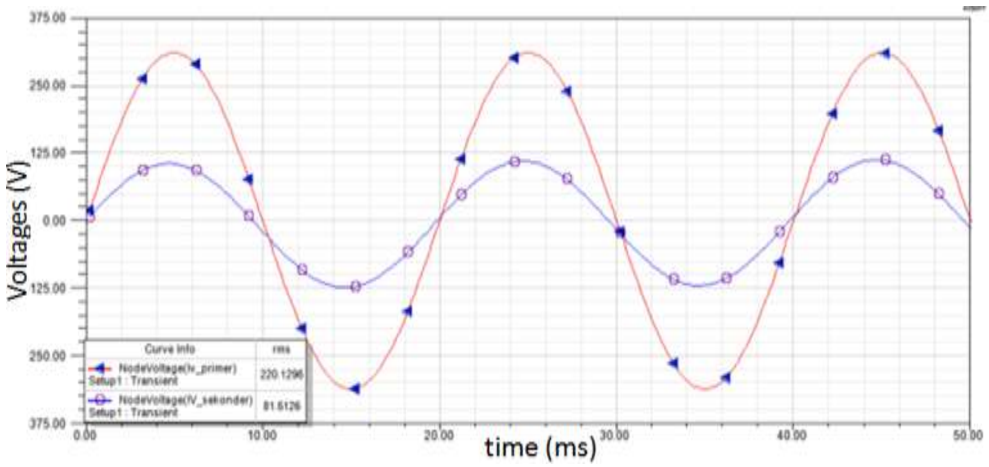

Figure 14. Voltages in no-load operation

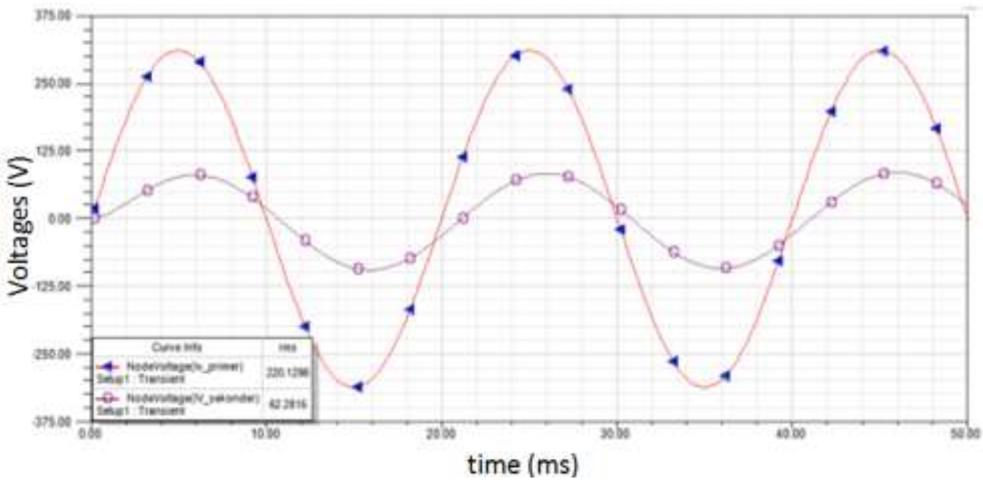

Figure 15.Voltages in full load operation

3.3. Experimental Results

Experimental setup is shown in Figure 7. Input power is measured by wattmeter and charging current and voltage are measured by multi meters. Results are given in Table 2. for full load and no load operation.

Table 2. No load and full load experiments

operation mode	air gap (mm)	Primary		Secondary	
		Voltage (V)	Current (A)	Voltage (V)	Current (A)
No-Load	0	226	0,32	130,4	0
	3	226	3,33	103	0
	5	226	4,4	85	0
Full Load	0	226	5	84	8
	3	226	4,48	63	4,24
	5	226	5,33	54	4,03

Increasing of air gap distance is decreased secondary voltage and current, primary current is increased. For this reason transferred power and efficiency is lower due to larger air gap.This transformer was used in WCS system to charge empty battery group which is serial connected 4 lead acid batteries (12 V 14Ah). WCS is transferred energy for about 45 minutes from 3 mm airgap. During this time, average63 V voltage and 4.24 A current are applied to battery group by WCS and about 200 Wh energy is transferred wirelessly. Winding temperature is observed and shown in Figure 16. Temperature is fixed as 132 Celcius degree after 45 minutes. WCS is not equipped cooling system. A cooling fan can be used.

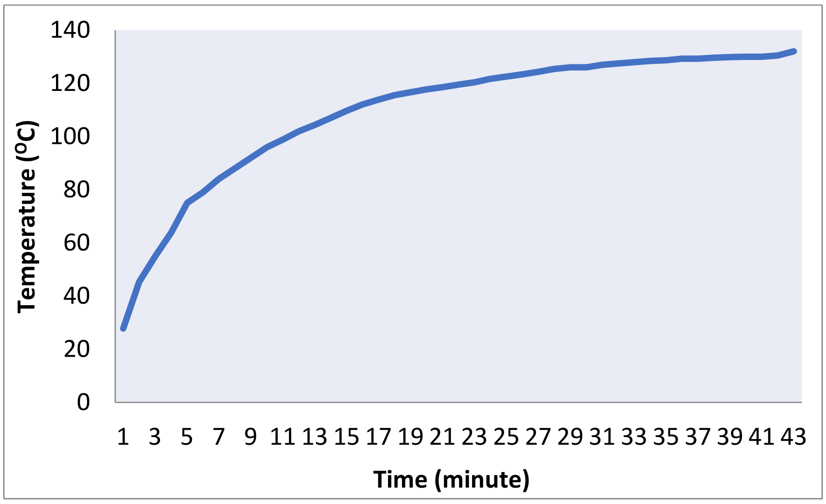

Figure 16. Time-temperature graph

4. Conclusion

Performance tests of EE structured air gapped transformer which is designed for wireless charging of battery group at network frequency were performed with the finite element analysis and experiments. No load, full load and short circuit operating conditions were simulated according to the variations of air gap distance. Air gap distance gets longer, transformer's efficiency, power factor, secondary terminal voltage and secondary current are reduced and primer current is increased. In the case where the air gap is zero while efficiency is about %70 in the case of this distance is 5mm efficiency decreases to about %25. Air gapped transformers were used in WCS and tested. About 63 V voltage and 4.24 A current are applied to battery group by WSC and 200 Wh energy is transferred wirelessly along 45 minutes. The charging system works under the network frequency and has low cost. When air gap distance increases, system efficiency is reduced. In order to increase this efficiency it is necessary to transfer power with high frequency. This is an additional cost for that also requires a high frequency inverter. This system is suitable for wireless charging in short air gap distance so it is simple and cheap solution for charging of shuttle robots.

Acknowledgements

This study was presented in EEB2016 Symposium and published in proceeding in Turkish. This paper is extended version of same study in English. It is supported by DIMAK Co. Ltd. in the Tokat Technology Development Zone.

Journal of New Results in Science 12(2016) 159-169

References

[1] H. Takanashi, Y. Sato, Y. Kaneko, S. Abe, and T. Yasuda, *A Large Air Gap 3 kW Wireless Power Transfer System for Electric Vehicles*, Energy Conversion Congress and Exposition (ECCE), (2012) pp: 269-274.

[2] S. Li, M, Chris, *Wireless Power Transfer for Electric Vehicle Applications*, IEEE Journal of Emerging and Selected Topics in Power Electronics, (2015) Volume: 3(1) pp: 4-17.

[3] M. Bloom, G. Niu, *Design Considerations for Wireless Electric Vehicle Charging*, Transportation Electrification Conference and Expo (ITEC), (2013) pp: 1-6.